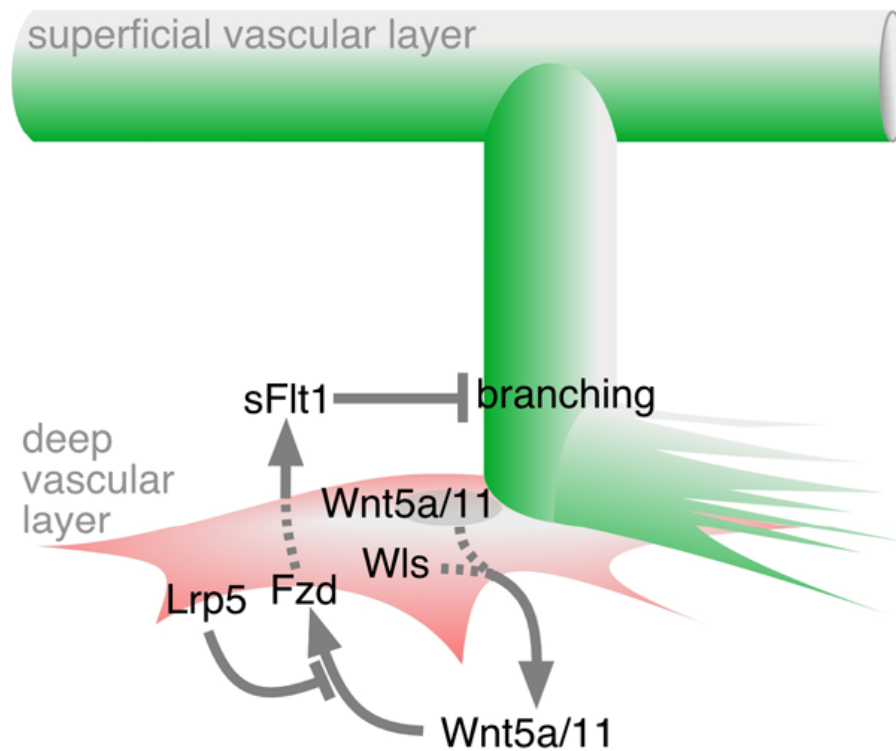
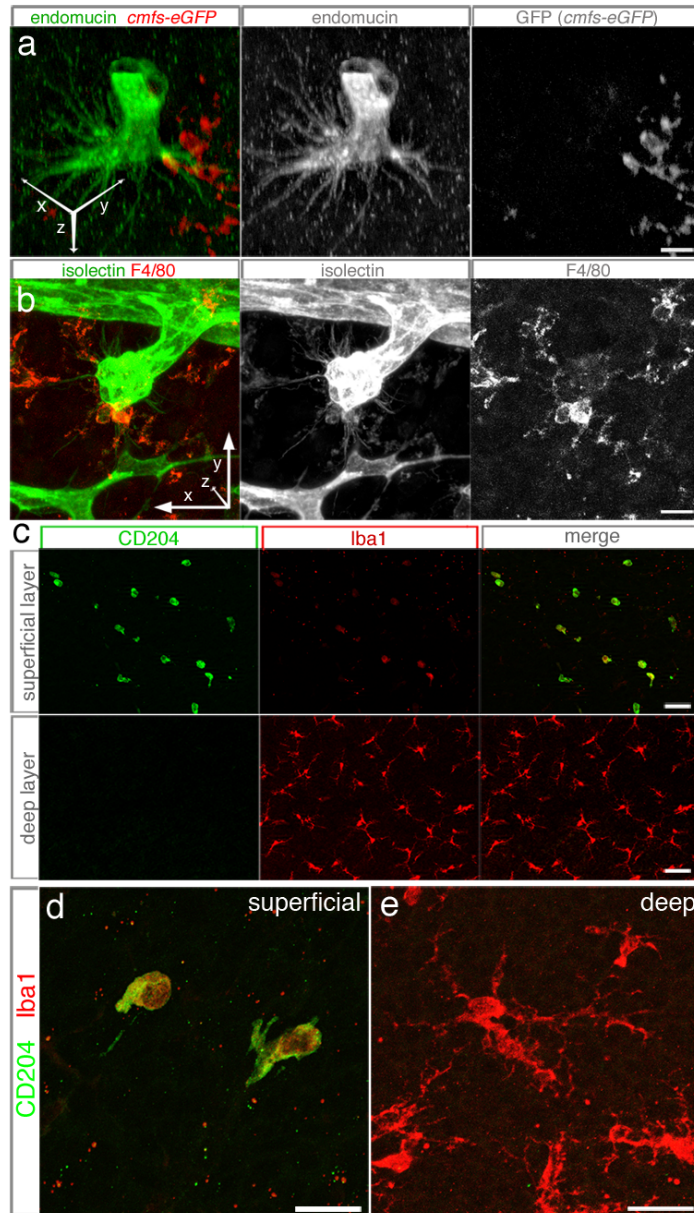


## Supplemental Figures and Legends

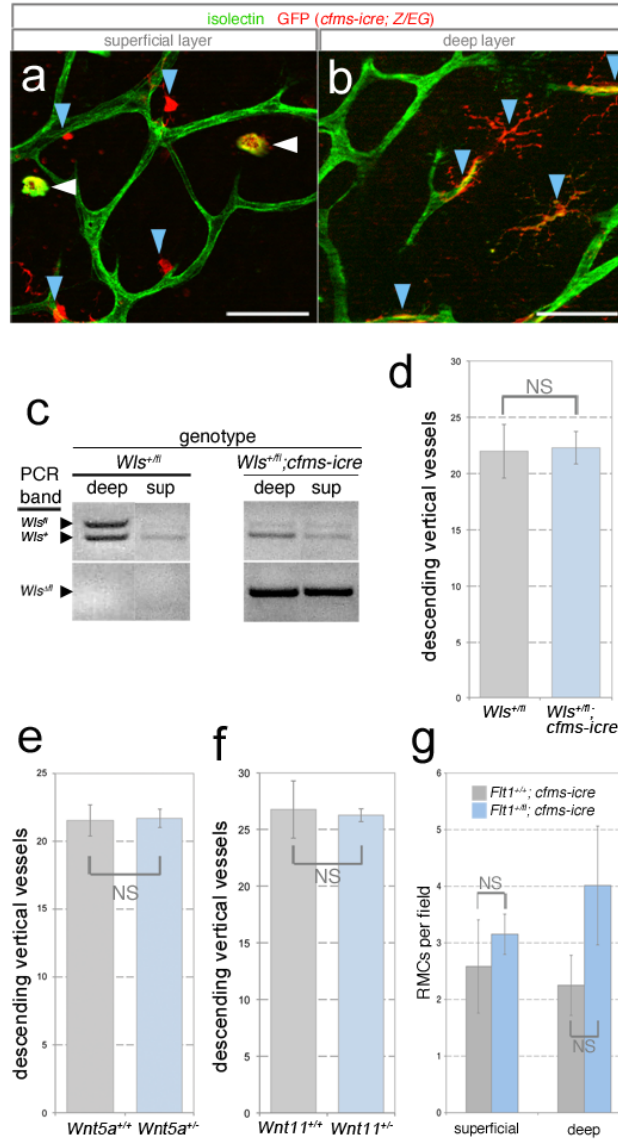


**Supplementary Figure 1. Schematic depicting suppression of angiogenic branching by a Wnt-Flt1 pathway in deep layer RMCs.** Our analysis supports a model in which RMCs (red) suppress angiogenic branching in the deep retinal layer using a Wnt-Flt1 pathway. *Wnt5a* and *Wnt11* are expressed in deep layer RMCs. When their function is compromised either by heterozygous germ-line mutation or by RMC deletion of the Wnt ligand transporter Wntless (Wls), the consequence is additional branching at the point of contact between angiogenic sprouts (green) and RMCs. A role for the canonical Wnt pathway coreceptor Lrp5 in suppression of the non-canonical Wnt response is suggested by the hypovascularization that arises with RMC conditional deletion of Lrp5. Based on a phenocopy of the conditional *Wls* phenotype with conditional *Flt1* deletion, and the loss of the *Flt1* transcript with RMC *Wls* mutation, we argue that a Wnt pathway normally enhances *Flt1* expression. In turn, we suggest that Flt1 suppresses angiogenic branching, presumably through suppression of VEGF activity.



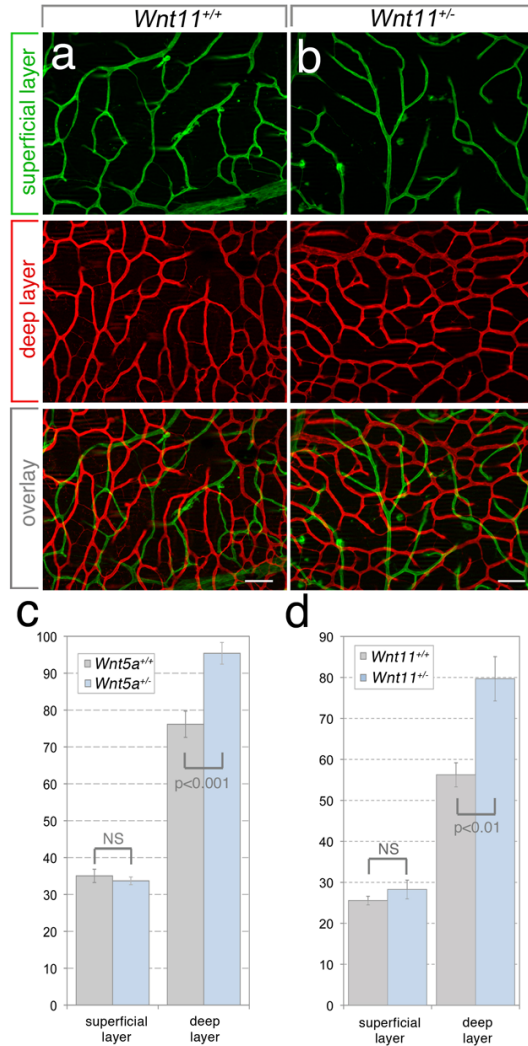
### Supplementary Figure 2. Deep layer RMCs interact with angiogenic tip cells

(a) 3D reconstruction of double labeling for endomucin (green and grey) and GFP (red and grey) in the *cfms-eGFP* mouse line<sup>1</sup> reveals the interaction of angiogenic tip cells and RMCs at the outer edge of the retinal inner nuclear layer. (b) 3D reconstruction of double labeling for isolectin (green and grey) and F4/80<sup>2</sup> (red and grey) shows an angiogenic tip cell above an F4/80 labeled RMC in the deep vascular layer. According to these markers, the processes of each cell type are distinct morphologically. The filopodial processes of angiogenic tip cells are long and thin while the processes of RMCs are lobular. Using labelling with isolectin (VECs and RMCs) and F4/80 (RMCs) we confirmed the close interaction between tip cells and RMCs in the deep retinal layer. Scale bars are 5  $\mu\text{m}$ . (c-e) Expression of CD204 (green) and Iba1 (red) in RMCs at the location of the superficial and deep vascular layers (c) and at higher magnification (d, e). Deep layer RMCs also express CD11b<sup>3</sup>. CD204, F4/80 and CD11b surface markers were used to cell sort RMC populations. Scale bars are 50  $\mu\text{m}$  (c) and 20  $\mu\text{m}$  (d, e).



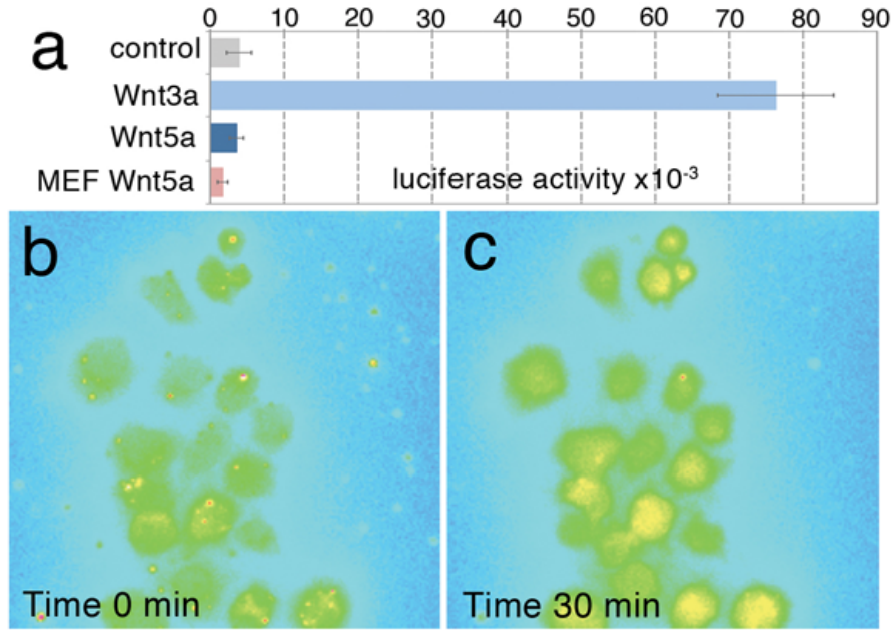
**Supplementary Figure 3. Supplementary data on *Wis<sup>fl</sup>* allele conversion, number of descending vertical sprouts, and RMC numbers.**

(a, b) The *cfms-icre* transgene is active in myeloid cells<sup>4</sup> and when crossed with the cre reporter *Z/EG*<sup>5</sup>, GFP expression in the P12 retina is found in both superficial and deep RMCs. Isolectin (green) and anti-GFP labeling (red) of superficial (a) and deep (b) vascular layers in a P12 *Z/EG; cfms-icre* retina. Retinal myeloid cells with both amoeboid (a) and extended (b) morphologies are GFP-positive (arrowheads). Some myeloid cell are also isolectin positive (white arrowheads). There is no indication that this cre driver converts *Z/EG* in other cell types. Scale bars are 50  $\mu$ m. (c) P12 deep RMCs (deep) and superficial RMCs (sup) were flow sorted and then genotyped by PCR to show that the recombined *Wis<sup>fl</sup>* allele could be detected only in the *cfms-icre* genotypes. (d, e, f) Quantification of vertical vessels connecting into the deep layer in *Wis<sup>fl/fl</sup>* and *Wis<sup>fl/fl</sup>; cfms-icre* mice (n=8)(d), in *Wnt5a<sup>+/+</sup>* and *Wnt5a<sup>+/-</sup>* mice (n=10)(e), and in *Wnt11<sup>+/+</sup>* and *Wnt11<sup>+/-</sup>* mice (n=4)(f). (g) Quantification of the number of deep RMCs per microscope field at P18 in *Flt1<sup>+/fl</sup>* and *Flt1<sup>+/fl</sup>; cfms-icre* mice. n=7. Student's T-test was used to determine statistical significance. Error bars are s.e.m. NS – Not significant.



**Supplementary Figure 4. *Wnt5a* and *Wnt11* heterozygote mice show a deep layer vascular overgrowth.**

Wls is believed to function as a Wnt ligand-specific transporter<sup>6</sup>. However, since it was possible that it had additional functions besides Wnt ligand transport, we assessed the phenotype of gene-targeted mice with loss-of-function mutations in Wnt ligand genes. Of the ligands expressed in myeloid cells, we analyzed gene targeted mice for *Wnt5a*<sup>7</sup> and *Wnt11*<sup>8</sup>. Since both show perinatal lethality as homozygotes, we examined heterozygotes for defects in retinal vascularization. (a, b) Isolectin labeling of superficial (green) and deep (red) vasculature in the retina of *Wnt11*<sup>+/+</sup> (a) and *Wnt11*<sup>+/-</sup> (b) mice. Scale bars are 50  $\mu$ m. (c, d) Quantification of vessel branch points in superficial and deep vasculature of *Wnt5a* (n=10)(c) and *Wnt11* (n=4)(d) control and experimental mice. Consistent with a role for each ligand in an angiogenesis suppression pathway, *Wnt11* heterozygotes and *Wnt5a* heterozygotes both showed increased vascular density in the deep vascular layer at P18. Both the *Wnt5a* and *Wnt11* heterozygous phenotypes were milder than those observed in the *Wls* conditional heterozygote, as might be expected. Neither showed any significant change in the density of the superficial vascular layer nor in the number of vertical connections between the superficial and deep vascular layers (see Fig S2). For (c) and (d) a Student's T-test (two-tailed) was used to determine statistical significance. All error bars are s.e.m. NS – Not significant.



**Supplementary Figure 5. Wnt5a does not elicit a canonical response but activates a Ca<sup>2+</sup> response in myeloid-like cells.**

(a) Luciferase activity on SuperTopFlash cells with Wnt3a, Wnt5a, or Wnt5a-transfected MEF supernatant. For Wnt3a,  $p < 0.001$ .  $n = 4$ . (b, c) Intracellular Ca<sup>2+</sup> in RAW264.7 cells before (b) and after (c) Wnt5a exposure.

## Supplementary References

- 1 Sasmono, R. T. *et al.* A macrophage colony-stimulating factor receptor-green fluorescent protein transgene is expressed throughout the mononuclear phagocyte system of the mouse. *Blood* **101**, 1155-1163., (2003).
- 2 Hume, D. A. & Gordon, S. Mononuclear phagocyte system of the mouse defined by immunohistochemical localization of antigen F4/80. Identification of resident macrophages in renal medullary and cortical interstitium and the juxtaglomerular complex. *J. Exp. Med* **157**, 1704-1709, (1983).
- 3 Mendes-Jorge, L. *et al.* Scavenger function of resident autofluorescent perivascular macrophages and their contribution to the maintenance of the blood-retinal barrier. *Invest Ophthalmol Vis Sci* **50**, 5997-6005, (2009).
- 4 Deng, L. *et al.* A novel mouse model of inflammatory bowel disease links mammalian target of rapamycin-dependent hyperproliferation of colonic epithelium to inflammation-associated tumorigenesis. *Am J Pathol* **176**, 952-967, (2010).
- 5 Novak, A., Guo, C., Yang, W., Nagy, A. & Lobe, C. G. Z/EG, a double reporter mouse line that expresses enhanced green fluorescent protein upon Cre-mediated excision. *Genesis* **28**, 147-155, (2000).
- 6 Ching, W. & Nusse, R. A dedicated Wnt secretion factor. *Cell* **125**, 432-433, (2006).
- 7 Yamaguchi, T. P., Bradley, A., McMahon, A. P. & Jones, S. A Wnt5a pathway underlies outgrowth of multiple structures in the vertebrate embryo. *Development* **126**, 1211-1223., (1999).
- 8 Majumdar, A., Vainio, S., Kispert, A., McMahon, J. & McMahon, A. P. Wnt11 and Ret/Gdnf pathways cooperate in regulating ureteric branching during metanephric kidney development. *Development* **130**, 3175-3185., (2003).